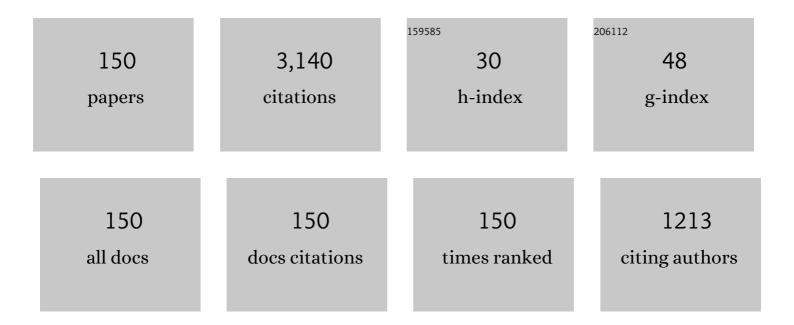
List of Publications by Year in descending order

Source: https://exaly.com/author-pdf/6860935/publications.pdf Version: 2024-02-01



LOSEDH NUSEN

#	Article	IF	CITATIONS
1	Gain Saturation Regime for Laser-Driven Tabletop, Transient Ni-Like Ion X-Ray Lasers. Physical Review Letters, 2000, 84, 4834-4837.	7.8	187
2	Prepulse technique for producing low-ZNe-like x-ray lasers. Physical Review A, 1993, 48, 4682-4685.	2.5	162
3	A Saturated X-ray Laser Beam at 7 Nanometers. Science, 1997, 276, 1097-1100.	12.6	141
4	Demonstration of a narrow-divergence x-ray laser in neonlike titanium. Physical Review A, 1990, 42, 6962-6965.	2.5	102
5	Demonstration of Saturation in a Ni-like Ag X-Ray Laser at 14 nm. Physical Review Letters, 1997, 78, 3856-3859.	7.8	99
6	Dielectronic satellite spectra for helium-like ions. Atomic Data and Nuclear Data Tables, 1988, 38, 339-379.	2.4	74
7	A measurement of the equation of state of carbon envelopes of white dwarfs. Nature, 2020, 584, 51-54.	27.8	70
8	X-ray scattering measurements on imploding CH spheres at the National Ignition Facility. Physical Review E, 2016, 94, 011202.	2.1	64
9	Laser with dynamic holographic intracavity distortion correction capability. Applied Physics Letters, 1982, 41, 219-220.	3.3	61
10	Bursts of Terahertz Radiation from Large-Scale Plasmas Irradiated by Relativistic Picosecond Laser Pulses. Physical Review Letters, 2015, 114, 255001.	7.8	60
11	Nearly Monochromatic Lasing at 182 â,,« in Neonlike Selenium. Physical Review Letters, 1995, 74, 3376-3379.	7.8	57
12	Saturated output of a GeXXIII x-ray laser at 19.6 nm. Physical Review A, 1996, 54, R4653-R4656.	2.5	55
13	Probing matter at Gbar pressures at the NIF. High Energy Density Physics, 2014, 10, 27-34.	1.5	52
14	Wavelengths of neon-like 3p→ 3sX-ray laser transitions. Physica Scripta, 1994, 49, 588-591.	2.5	50
15	An ultrahighâ€Qisotropically sensitive optical filter employing atomic resonance transitions. Journal of Applied Physics, 1979, 50, 610-614.	2.5	49
16	Lasing at 79 nm in nickellike neodymium. Optics Letters, 1995, 20, 1386.	3.3	49
17	Demonstration of transient gain x-ray lasers near 20??nm for nickellike yttrium, zirconium, niobium, and molybdenum. Optics Letters, 1999, 24, 101.	3.3	47
18	Sensitivity of lasing in neonlike zinc at 212 nm to the use of the prepulse technique. Optics Letters, 1995, 20, 374.	3.3	44

#	Article	IF	CITATIONS
19	Longitudinal coherence measurements of a transient collisional x-ray laser. Optics Letters, 2003, 28, 2261.	3.3	44
20	Traveling wave excitation and amplification of neon-like germanium 3p–3s transitions. Optics Communications, 1994, 110, 585-589.	2.1	43
21	Wavelengths of the Ni-like4d1S0–4p1P1x-ray laser line. Physical Review A, 1998, 58, R2668-R2671.	2.5	41
22	Dielectronic-recombination-rate coefficients for neonlike ions. Physical Review A, 1986, 33, 264-268.	2.5	40
23	Absolute Equation-of-State Measurement for Polystyrene from 25 to 60ÂMbar Using a Spherically Converging Shock Wave. Physical Review Letters, 2018, 121, 025001.	7.8	39
24	Soft-x-ray lasing at 32.6 nm in Ne-like Ti ions driven by 40 J of energy from two 650-ps laser pulses. Physical Review A, 1996, 53, 3640-3646.	2.5	37
25	COMPARISON OF SATELLITE SPECTRA FOR H-LIKE Fe AND He-LIKE Fe, Ca, AND S CALCULATED BY THREE DIFFERENT METHODS. Atomic Data and Nuclear Data Tables, 1997, 67, 225-329.	2.4	37
26	Damage and ablation of large bandgap dielectrics induced by a 469 nm laser beam. Optics Letters, 2006, 31, 68.	3.3	36
27	Dielectronic satellite spectra for hydrogen-like ions. Atomic Data and Nuclear Data Tables, 1987, 37, 191-233.	2.4	35
28	Atomic Number Scaling of the Nickel-Like Soft X-Ray Lasers. International Journal of Modern Physics B, 1997, 11, 945-990.	2.0	33
29	Gain saturation of the Ni-like X-ray lasers. Optics Communications, 1998, 158, 55-60.	2.1	33
30	Reinvestigating the early resonantly photopumped x-ray laser schemes. Applied Optics, 1992, 31, 4950.	2.1	32
31	Narrow-band optical filter through phase conjugation by nondegenerate four-wave mixing in sodium vapor. Optics Letters, 1981, 6, 380.	3.3	31
32	Lasing on the self-photopumped nickel-like4f1P1→4d1P1x-ray transition. Physical Review A, 1999, 60, R2677-R2680.	2.5	30
33	Understanding the effects of radiative preheat and self-emission from shock heating on equation of state measurement at 100s of Mbar using spherically converging shock waves in a NIF hohlraum. Matter and Radiation at Extremes, 2020, 5, .	3.9	29
34	Equation of state of boron nitride combining computation, modeling, and experiment. Physical Review B, 2019, 99, .	3.2	28
35	Measurements of line overlap for resonant spoiling of x-ray lasing transitions in nickel-like tungsten. Physical Review A, 1995, 52, 2689-2692.	2.5	27
36	Ni-like x-ray lasers resonantly photopumped by Ly-α radiation. Physical Review Letters, 1991, 66, 305-308.	7.8	26

#	Article	IF	CITATIONS
37	Measurement of the Ly-α Mg resonance with the 2s→3pNe-like Ge line. Physical Review A, 1994, 50, 2143-2149.	2.5	26
38	Dielectronic satellite spectra for neon-like ions. Atomic Data and Nuclear Data Tables, 1989, 41, 131-177.	2.4	25
39	Analysis of the resonantly photopumped Na-Ne x-ray-laser scheme. Physical Review A, 1991, 44, 4591-4598.	2.5	25
40	Study of Ne- and Ni-like x-ray lasers using the prepulse technique. Physics of Plasmas, 1997, 4, 479-489.	1.9	25
41	Absolute Hugoniot measurements from a spherically convergent shock using x-ray radiography. Review of Scientific Instruments, 2018, 89, 053505.	1.3	24
42	Measurement of line overlap for resonant photopumping of transitions in neonlike ions by nickel-like ions. Physical Review A, 1993, 47, 1403-1406.	2.5	23
43	Lasing on the 3d→3pneonlike x-ray laser transitions driven by a self-photo-pumping mechanism. Physical Review A, 1996, 53, 4539-4546.	2.5	23
44	Analysis of a picosecond-laser-driven Ne-like Ti x-ray laser. Physical Review A, 1997, 55, 3271-3274.	2.5	23
45	Theoretical and experimental investigation of the equation of state of boron plasmas. Physical Review E, 2018, 98, 023205.	2.1	23
46	Dielectronic Structure of 2l–1sTransitions of Multicharged Ions of Argon with Nuclear ChargesZ=10-17. Physica Scripta, 2000, 61, 555-566.	2.5	22
47	The dielectronic satellites to the 2s-3pNe-like krypton resonance lines. Physica Scripta, 1994, 50, 106-109.	2.5	21
48	Boron–carbide barrier layers in scandium–silicon multilayers. Thin Solid Films, 2004, 469-470, 372-376.	1.8	20
49	Plasmas with an index of refraction greater than 1. Optics Letters, 2004, 29, 2677.	3.3	20
50	Measurements of line overlap for resonant photopumping of 4→4 transitions in highly charged nickel-like ions. Physical Review A, 1992, 46, R25-R28.	2.5	19
51	Observation of hyperfine splitting on an x-ray laser transition. Physical Review Letters, 1993, 70, 3713-3716.	7.8	19
52	Self-photopumped neonlike x-ray laser. Optics Letters, 1996, 21, 408.	3.3	19
53	High-resolution measurement, line identification, and spectral modeling of the KÎ' spectrum of heliumlike argon emitted by a laser-produced plasma using a gas-puff target. Physical Review E, 1997, 55, 3773-3776.	2.1	19
54	The x-ray emission spectra of multicharged xenon ions in a gas puff laser-produced plasma. Journal of Physics B: Atomic, Molecular and Optical Physics, 1999, 32, 113-122.	1.5	19

#	Article	IF	CITATIONS
55	Demonstration of a neonlike argon soft-x-ray laser with a picosecond-laser-irradiated gas puff target. Optics Letters, 2001, 26, 1403.	3.3	18
56	Neon-like X-ray lasers of zirconium, niobium and bromine. Journal of Physics B: Atomic, Molecular and Optical Physics, 1993, 26, L243-L247.	1.5	17
57	Use of the prepulse technique to enhance the weak 182-nm laser line in neonlike selenium. Optics Letters, 1994, 19, 1137.	3.3	16
58	Two-dimensional spatial imaging of the multiple-pulse-driven 196-â,,« neonlike germanium x-ray laser. Physical Review A, 1997, 55, 827-830.	2.5	16
59	Z dependences of the energy levels and autoionization rates for 213I' states of two-electron systems. Journal of Physics B: Atomic, Molecular and Optical Physics, 1990, 23, 4451-4467.	1.5	15
60	Developing quartz and molybdenum as impedance-matching standards in the 100-Mbar regime. Physical Review B, 2019, 99, .	3.2	15
61	A tunable narrowband optical filter via phase conjugation by nondegenerate four-wave mixing in a doppler-broadened resonant medium. Optics Communications, 1981, 39, 199-204.	2.1	14
62	Nondegenerate four-wave mixing in a homogeneously broadened two-level system with saturating pump waves. IEEE Journal of Quantum Electronics, 1982, 18, 1947-1952.	1.9	14
63	Resonantly photopumped Ni-like Er x-ray laser. Physical Review A, 1989, 40, 5440-5443.	2.5	14
64	An argon-pumped yttrium X-ray laser. Physica Scripta, 1993, 47, 42-44.	2.5	14
65	Two-dimensional near-field images of the neonlike germanium soft-x-ray laser. Optics Letters, 1996, 21, 866.	3.3	14
66	Near-field spatial imaging of a Ni-like Ag 140-Ã x-ray laser. Physical Review A, 1997, 56, 3161-3165.	2.5	14
67	Dielectronic recombination rate coefficients for hydrogen-like ions. Journal of Quantitative Spectroscopy and Radiative Transfer, 1986, 36, 539-545.	2.3	13
68	Resonantly photo-pumped Na-like X-ray lasers. Journal of Quantitative Spectroscopy and Radiative Transfer, 1992, 47, 171-177.	2.3	13
69	Inner-Shell transitions of Be-like ions withZ= 6–54. Physica Scripta, 1995, 51, 589-593.	2.5	13
70	Relative merits of using curved targets and the prepulse technique to enhance the output of the neon-like germanium X-ray laser. Optics Communications, 1996, 124, 287-291.	2.1	13
71	Spectra of multiply charged nickel and copper ions in an X-pinch plasma. Quantum Electronics, 1993, 23, 397-405.	1.0	12
72	The observation of the Ne-like ion resonance line satellites for Cr XV ··· Ni XIX CO2-laser produced plasma. Physica Scripta, 1994, 50, 102-105.	2.5	12

#	Article	IF	CITATIONS
73	Autoionization states of lithium-like ions with large principal quantum number. Journal of Quantitative Spectroscopy and Radiative Transfer, 1994, 51, 853-874.	2.3	12
74	Study of lasing in low-Zneon-like ions using the prepulse technique. Physica Scripta, 1995, 52, 158-161.	2.5	12
75	Z-dependences of the atomic characteristics for 1s2l2l′ states of three electron systems. Journal of Quantitative Spectroscopy and Radiative Transfer, 1993, 49, 371-381.	2.3	11
76	High-resolution measurements of Mg xi and Cu xx resonance and satellite transitions and the resonance defect in the Mg-pumped Cu x-ray laser scheme. Physical Review A, 1995, 52, 3644-3650.	2.5	11
77	Photo-pumping resonance for modifying the kinetics of a neonlike La47+laser. Physica Scripta, 1995, 51, 322-325.	2.5	11
78	Impact of anomalous dispersion on the interferometer measurements of plasmas. Journal of Quantitative Spectroscopy and Radiative Transfer, 2006, 99, 425-438.	2.3	11
79	Multiply ionized carbon plasmas with index of refraction greater than one. Laser and Particle Beams, 2007, 25, 47-51.	1.0	11
80	Modelling K shell spectra from short pulse heated buried microdot targets. High Energy Density Physics, 2017, 23, 178-183.	1.5	11
81	Resonantly photo-pumped Li-like x-ray lasers. Applied Optics, 1992, 31, 4957.	2.1	10
82	Reinterpretation of the neon-like titanium laser experiments. Optical Engineering, 1994, 33, 2687.	1.0	10
83	Resonant-line overlap for photopumping and spoiling of x-ray lasing transitions in neonlike Fe xvii and Cu xx. Physical Review A, 1994, 49, 3123-3126.	2.5	10
84	X-ray lasers as sources for resonance-fluorescence experiments. Applied Physics B: Lasers and Optics, 1994, 58, 7-11.	2.2	10
85	Oscillator strengths of the first forbidden lines of rubidium. Journal of Quantitative Spectroscopy and Radiative Transfer, 1978, 20, 327-329.	2.3	9
86	A Ne-like Cu laser resonantly photo-pumped by a He-like Mg line. Optics Communications, 1990, 78, 51-57.	2.1	9
87	Z-dependences of the energy levels and autoionization rates for 2141′ states of two electron systems. Journal of Quantitative Spectroscopy and Radiative Transfer, 1992, 48, 61-78.	2.3	9
88	Measurements of 3d-5fand 3d-6ftransition energies in nickel-like ions for resonant photopumping by helium-like ions. Physica Scripta, 1994, 49, 556-560.	2.5	9
89	Hyperfine splittings of neonlike lasing lines. Physical Review A, 1994, 49, 2381-2388.	2.5	9
90	Transitions from Na-like and Mg-like autoionizing levels of multicharged molybdenum ions in an X-pinch plasma. Physica Scripta, 1995, 51, 454-458.	2.5	9

#	Article	IF	CITATIONS
91	Transient collisional excitation X-ray lasers with 1-ps tabletop drivers. IEEE Journal of Selected Topics in Quantum Electronics, 1999, 5, 1441-1446.	2.9	9
92	Near-field spatial imaging of the Ni-like palladium soft-X-ray laser. Optics Communications, 2002, 210, 305-312.	2.1	9
93	Localization and Screening Enhancement in Asymmetric Binary Ionic Mixtures. Contributions To Plasma Physics, 2015, 55, 413-420.	1.1	9
94	Modeling the gain of inner-shell X-ray laser transitions in neon, argon, and copper driven by X-ray free electron laser radiation using photo-ionization and photo-excitation processes. Matter and Radiation at Extremes, 2016, 1, 76-81.	3.9	9
95	A 33 angstrom laboratory X-ray laser. Optics Communications, 1989, 72, 371-376.	2.1	8
96	Vanadium-pumped titanium x-ray laser. Optics Letters, 1990, 15, 798.	3.3	8
97	An Ne-like Fe laser resonantly photo-pumped by Ne X Ly-α radiation. Journal of Quantitative Spectroscopy and Radiative Transfer, 1991, 46, 547-556.	2.3	8
98	Resonantly photo-pumped Ni-like TI X-ray laser. Physica Scripta, 1991, 43, 596-598.	2.5	8
99	Precision measurements of the wavelengths of spectral lines of multiply charged krypton and argon ions formed in a gas target heated by laser radiation. Quantum Electronics, 1997, 27, 691-695.	1.0	8
100	Reminiscing about the early years of the X-ray laser. Quantum Electronics, 2003, 33, 1-2.	1.0	8
101	Observation of multiply ionized plasmas with dominant bound electron contribution to the index of refraction. Journal of Quantitative Spectroscopy and Radiative Transfer, 2006, 99, 165-174.	2.3	8
102	A 64 à Ne-like Ge X-ray laser resonantly photo-pumped by Ly-α Mg radiation. Optics Communications, 1994, 108, 283-288.	2.1	7
103	Energies of neon-liken= 4 ton= 2 resonance lines. Physica Scripta, 1996, 54, 183-187.	2.5	7
104	Mo:Y multilayer mirror technology utilized to image the near-field output of a Ni-like Sn laser at 119nm. Optics Letters, 2003, 28, 2249.	3.3	7
105	Understanding the anomalous dispersion of doubly ionized carbon plasmas near 47nm. High Energy Density Physics, 2008, 4, 107-113.	1.5	7
106	Using neutrons to measure keV temperatures in highly compressed plastic at multi-Gbar pressures. High Energy Density Physics, 2016, 21, 20-26.	1.5	7
107	Observation of He-like Satellite Lines of the H-like Potassium K xix Emission. Astrophysical Journal, 2019, 881, 92.	4.5	7
108	X-ray Thomson scattering measurements from hohlraum-driven spheres on the OMEGA laser. Review of Scientific Instruments, 2016, 87, 11E724.	1.3	6

#	Article	IF	CITATIONS
109	Benchmarking boron carbide equation of state using computation and experiment. Physical Review E, 2020, 102, 053203.	2.1	6
110	Z-dependences of the atomic characteristics for selected 2l4l' states. Journal of Quantitative Spectroscopy and Radiative Transfer, 1990, 43, 445-450.	2.3	5
111	17-nm rubidium-ion laser. Optics Letters, 1992, 17, 1518.	3.3	5
112	Lspectra of zinc ions in the wavelength region 0.65–1.18 nm observed in a plasma heated by a Nd laser. Quantum Electronics, 1993, 23, 1010-1025.	1.0	5
113	Space-resolved investigation of lasing on the two J = 0â^'1, 3p-3s transitions at 20.5 and 25.5 nm in neon-like iron. Optics Communications, 1995, 119, 557-562.	2.1	5
114	Measurement of the 3d-4ftransition in Ni-like Er for use in a photopumped x-ray-laser scheme. Physical Review A, 1995, 51, 1683-1686.	2.5	5
115	Theoretical analysis of the Doubly Excited 3Inl' States of Sodiumlike Copper. Physica Scripta, 1998, 57, 334-344.	2.5	5
116	The role of EBIT in X-ray laser research. Canadian Journal of Physics, 2008, 86, 19-23.	1.1	5
117	Self-photopumped x-ray lasers from elements in the Ne-like and Ni-like ionization state. Optics Communications, 2017, 382, 288-293.	2.1	5
118	Use of a laser plasma in determination of a resonance defect of the Lyα1,2lines of Mg XII and the 2s—3p lines of Ge XXIII. Quantum Electronics, 1994, 24, 133-137.	1.0	4
119	Comparison of autoionization rates for 3131' states of two electron systems. Journal of Quantitative Spectroscopy and Radiative Transfer, 1994, 52, 729-741.	2.3	4
120	Optimisation of drive pulse configuration for a Ni-like Sn X-ray laser at 12 nm. Physics Letters, Section A: General, Atomic and Solid State Physics, 1997, 234, 410-414.	2.1	4
121	NEW COMPREHENSIVE THEORETICAL ANALYSIS OF THE DOUBLY EXCITED STATES OF SODIUM-LIKE IRON. Journal of Quantitative Spectroscopy and Radiative Transfer, 1998, 60, 605-622.	2.3	4
122	Using the X-ray free-electron laser to drive a photo-pumped helium-like neon X-ray laser at 23Ânm. High Energy Density Physics, 2011, 7, 6-10.	1.5	4
123	The effect of bound states on X-ray Thomson scattering for partially ionized plasmas. High Energy Density Physics, 2013, 9, 388-391.	1.5	4
124	Average-atom calculations of bound-free and free-free cross sections in dense plasmas. Physical Review E, 2020, 102, 043209.	2.1	4
125	Resonant photoionization for sodiumlike selenium. Physical Review A, 1988, 38, 2167-2170.	2.5	3
126	The study of Na-like multiply-charged ion x-ray spectra excited by a pulsed laser plasma source. Physica Scripta, 1995, 52, 377-385.	2.5	3

#	Article	IF	CITATIONS
127	Study of anomalous lasing behavior on the twoJ=0?1 transitions in Ne-like V. Applied Physics B: Lasers and Optics, 1996, 63, 125-130.	2.2	3
128	Dielectronic satellites to the Ne-like yttrium resonance lines. Physica Scripta, 1996, 54, 240-249.	2.5	3
129	Measurement of spatial gain distribution for a neonlike germanium 196-nm laser. Optics Letters, 1997, 22, 1320.	3.3	3
130	Scaling Laws for Electron Densities and Gain Coefficients in Low-ZNe-like Lasers. Physica Scripta, 1998, 57, 237-241.	2.5	3
131	Dielectronic Recombination for F-like and Ne-like Ions. Physica Scripta, 1998, 58, 203-219.	2.5	3
132	Studies on collisional pumping of soft X-ray lasers at ILE. IEEE Journal of Selected Topics in Quantum Electronics, 1999, 5, 1460-1468.	2.9	3
133	Resonant bound-free contributions to Thomson scattering of X-rays byÂwarm dense matter. High Energy Density Physics, 2013, 9, 407-409.	1.5	3
134	Precision measurements and identification of laser plasma emission spectra due to transitions from doubly excited levels of the sodium-like selenium ion. Measurement Techniques, 1994, 37, 477-492.	0.6	2
135	Investigation of gain and hyperfine splitting in the niobium X-ray laser. Applied Physics B: Lasers and Optics, 1994, 58, 3-5.	2.2	2
136	Simultaneous imaging of the near- and far-field intensity distributions of the Ni-like Sn X-ray laser. Applied Physics B: Lasers and Optics, 2004, 78, 971-974.	2.2	2
137	X-ray-line coincidence photopumping in a potassium-chlorine mixed plasma. Physical Review A, 2020, 101,	2.5	2
138	Comparison of ablators for the polar direct drive exploding pusher platform. High Energy Density Physics, 2021, 38, 100928.	1.5	2
139	Simultaneous compression and opacity data from time-series radiography with a Lagrangian marker. Review of Scientific Instruments, 2021, 92, 063514.	1.3	2
140	Z-dependences of atomic parameters of autoionization states of two-electron systems. Soviet Physics Journal (English Translation of Izvestiia Vysshykh Uchebnykh Zavedenii, Fizika), 1990, 33, 670-684.	0.0	1
141	Resonant photo-pumping of neon-like cobalt with sodium Ly- alpha radiation. Journal of Physics B: Atomic, Molecular and Optical Physics, 1994, 27, 4523-4529.	1.5	1
142	X-ray line coincidence photopumping in a solar flare. Monthly Notices of the Royal Astronomical Society, 2018, 474, 3782-3786.	4.4	1
143	Opacity of shock-heated boron plasmas. High Energy Density Physics, 2019, 31, 92-98.	1.5	1
144	Role of opacity at the 9 keV back lighter energy used in measuring the equation of state of boron at pressures up to a Gbar. High Energy Density Physics, 2020, 37, 100880.	1.5	1

#	Article	IF	CITATIONS
145	Designing a high-reflectivity normal-incidence Ge/Si multilayer X-ray mirror for the 44–50 nm wavelength range. OSA Continuum, 2020, 3, 3460.	1.8	1
146	Using neutrons and x rays to measure plasma conditions in a solid sphere of deuterated polyethylene compressed to densities of 35 g/cc at temperatures of 2 keV and pressures of 40 Gbar. Physics of Plasmas, 2021, 28, .	1.9	1
147	Dynamics of a multipleâ€pulseâ€driven xâ€ray laser plasma. Physics of Plasmas, 1996, 3, 606-613.	1.9	Ο
148	Using the XFEL to drive gain in L-shell systems using photoionization processes. , 2017, , .		0
149	Using the XFEL to Drive Gain in K-Shell and L-Shell Systems Using Photoionization and Photoexcitation of Inner Shell Transitions. Springer Proceedings in Physics, 2018, , 101-104.	0.2	0
150	Using distributions to understand neutron and x-ray production in ICF ignition capsules and other high energy density plasmas. Review of Scientific Instruments, 2021, 92, 123511.	1.3	0